

## Growth, Optical, Mechanical, Thermal and Dielectric Properties of Nonlinear Optical Single Crystal: Magnesium Iodate

S M RAVI KUMAR<sup>1\*</sup>, S SELVAKUMAR<sup>2</sup>, R GUNASEELAN<sup>3</sup>, G J SHANMUGA SUNDAR<sup>4</sup> and P SAGAYARAJ<sup>3</sup>

<sup>1</sup>PG & Research Department of Physics, Govt. Arts College, Thiruvannamalai 606 603, India

<sup>2</sup>Department of Physics, Govt. Arts & Science College, Nandanam, Chennai 600 035, India

<sup>3</sup>Department of Physics, Loyola College, Chennai 600 034, India

<sup>4</sup>Department of Physics, Arignar Anna Govt. Arts College, Cheyyar 604 407, India

(Received 27 June 2012; Revised 24 December 2012; Accepted 31 January 2013)

The good optical quality monometallic single crystals of magnesium iodate [Mg(IO<sub>3</sub>)<sub>2</sub>] were grown from aqueous solution by slow cooling technique at room temperature with dimension upto 7 x 6 x 3 mm<sup>3</sup> in the period of 25-30 days. Single crystal XRD analysis shows that magnesium iodate crystallizes in monoclinic system with space group P2<sub>1</sub>. The spectroscopic properties were characterized by FTIR and optical absorption spectra. Optical band gap is calculated as 3.96 eV. SHG efficiency is found to be around four times that of potassium dihydrogen phosphate (KDP) crystal. The microhardness test conducted on the crystal suggests that the crystal has a relatively high mechanical strength. TGA curve depict that the compound is thermally very stable up to 650°C. The dielectric constant and dielectric loss of the compound were measured at different temperature with varying frequencies.

**Key Words:** Solution Growth; Monometallic; Nonlinear Optical; Microhardness; TGA; Dielectric Constant

### 1. Introduction

Second order nonlinear optical (NLO) materials with short transparency cut off wavelength and stable physicochemical performances are needed in order to realize many of the applications like telecommunications, optical computing, optical information processing, optical disk data storage, laser remote sensing, laser-driven fusion, color displays and medical diagnostics [1-4]. Hence, considerable interest is given by the researchers in the synthesis of new materials which has excellent second order optical nonlinearities.

Though organic NLO crystals have high nonlinearities, fast response and tailor-made flexibility, their applications were limited because of their shortcomings such as poor physicochemical stability,

poor phase matching, red shift of the cut-off wavelength, etc. These problems have been solved by metal coordination ligands such as thiourea, thiocyanate and iodate. Some of the complex crystals like BTCE, ZTS, CMTC, MMTC, ZCTC, Hg(IO<sub>3</sub>)<sub>2</sub>, Cd(IO<sub>3</sub>)<sub>2</sub>, Mn(IO<sub>3</sub>)<sub>2</sub> [5-9] possess high nonlinearities as well as stable physicochemical properties. In view of this, we have initiated work on iodate complex crystals.

Metal iodates have been extensively studied for their nonlinear optical property due to the presence of a lone pair on iodine in the iodate group, which favours the acentric structure formation with remarkable thermal stability [10]. Thus, Bergman *et al.* in 1969 [10] has reported halate ions (IO<sub>3</sub><sup>-</sup>, BO<sub>3</sub><sup>-</sup>, ClO<sub>3</sub><sup>-</sup>) as potential candidates. Indeed, a very high

\*Author for Correspondence: E-mail: smravi78@rediffmail.com; Mobile: 09884473709

incidence of acentricity was found in metal iodates.

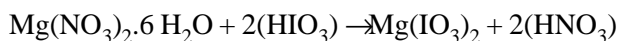
Metal iodates are interesting for infrared applications, as they are transparent from the visible part of the spectrum to the beginning of the far-infrared including the three atmospheric transparency window [11]. Furthermore, metal iodates seem particularly appropriate for several reasons. Their preparation is simple and reproducible. They are thermally stable at least up to 400°C. The transparency range of iodates is very large [12]. The crystal structure of  $M(\text{IO}_3)_2$  (where  $M = \text{Cd}, \text{Mg}, \text{Mn}, \text{Hg}, \text{Zn}, \text{Co}, \text{Ni}$ ) series of monometallic iodates have already been reported [11-13]. Although the structure of  $\text{Mg}(\text{IO}_3)_2$  was reported, the growth of bulk size crystal and their physical properties have not yet been studied. Single crystal XRD, UV-Vis-NIR, NLO test, thermal, microhardness, and dielectric studies of magnesium iodate (MGI) crystal were employed and reported. Optimum growth conditions were established by varying various parameters like pH, temperature, and concentration.

## 2. Experimental

### 2.1. Synthesis and Growth of MGI

Magnesium iodate salt was synthesized from high purity magnesium nitrate hexahydrate (AR grade) and iodic acid (AR grade) taken in the molar ratio 1:2. The stoichiometric amounts of the reactants were thoroughly dissolved in deionized water and stirred well. By adding a few drops of nitric acid into the solution a pH of 5 was maintained.

The chemical reaction is as follows:



The solution was filtered and covered with perforate lid. This was kept in a cryostat (accuracy 0.01°C) at 60°C to encourage the solution into evaporation. After 5 days, tiny crystals with good transparency were formed due to spontaneous nucleation, among them the defect free crystals were selected as seeds for growing bulk size crystals. The seeds were introduced in the filtered mother solution. Thereafter, attempts have been made to grow bulk

size crystals by slow cooling technique from 60 to 30°C. The MGI single crystal of size 7 x 6 x 3 mm<sup>3</sup> was grown in a period of 25-30 days. The photograph of as grown crystals of MGI is shown in Fig. 1. MGI crystal seems to be transparent, colourless and prismatic in shape with non-hygroscopicity in the open atmosphere.

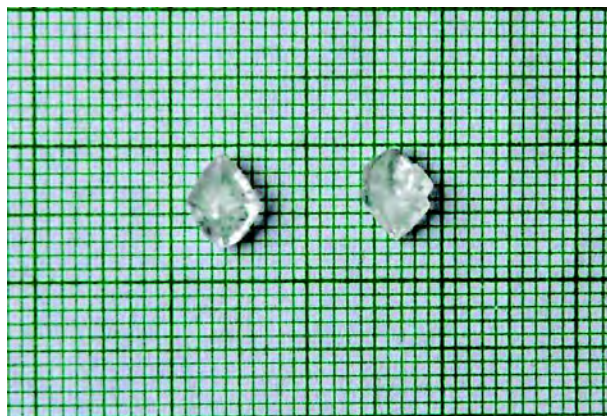


Fig. 1: Photograph of as grown crystals of MGI

### 2.2 Characterization

In order to obtain the crystal data of MGI crystals, single crystal X-ray diffraction studies were carried out using ENRAF NONIUS CAD4-F single X-ray diffractometer with  $\text{MoK}\alpha$  ( $\lambda = 0.717\text{\AA}$ ) radiation. The various functional groups present in MGI crystal were identified and confirmed by the FTIR study. The spectrum was recorded in the range 4000-450  $\text{cm}^{-1}$  using BRUKER IFS-66V spectrometer, by KBr pellet technique. The optical absorption spectrum was recorded in the range 200-2000 nm using VARIAN CARY 5E model UV-Vis-NIR spectrophotometer. The SHG effect was tested using a Nd:YAG, Q-switched laser. Microhardness study has been carried out using a Leitz Wetzlar Vickers microhardness tester fitted with a Vickers diamond pyramidal indenter attached to an incident light microscope. The thermo gravimetric analysis (TGA) and differential thermal analysis (DTA) of MGI crystal was carried out using ZETZSCH STA 409 C. The temperature dependent dielectric constant and dielectric loss of MGI were measured using HIOKI 3532 LCR HITESTER in the frequency range 100 Hz-5 MHz.

### 3. Results and Discussion

#### 3.1 Single Crystal XRD Studies

The title compound was analyzed by single crystal X-ray diffraction method to determine the unit cell parameters and space group. It is observed that the grown crystal crystallizes in the monoclinic system with non-centrosymmetric space group  $P2_1$  and unit cell parameters are  $a = 10.948 \text{ \AA}$ ,  $b = 5.182 \text{ \AA}$ ,  $c = 10.945 \text{ \AA}$  and volume =  $531.9 \text{ \AA}^3$ . The calculated density value is  $4.62 \text{ g/cm}^3$ . The XRD data of MGI is in good agreement with the reported value [14].

#### 3.2 FTIR Studies

Freshly crushed powder of MGI crystal was subjected to the Fourier Transform Infrared (FTIR) studies in order to analyze the functional groups present in the compound. The spectrum was recorded using BRUKER IFS -66V spectrometer KBr pellet technique in the range  $4000\text{--}450 \text{ cm}^{-1}$ . Fig. 2 shows the FTIR spectrum of magnesium iodate. The bands at  $2065$  and  $1021 \text{ cm}^{-1}$  are attributed to  $\gamma(\text{Mg-I})$  linked vibrations. The bands at  $762$  and  $705 \text{ cm}^{-1}$  are assigned to  $\gamma(\text{I=O})$  characteristics of mononuclear iodine compounds. The other vibrations present in the range  $700\text{--}800 \text{ cm}^{-1}$  are expected to have splitting vibration of iodates. The bands appeared in the recorded spectrum confirm the presence of iodate functional groups.

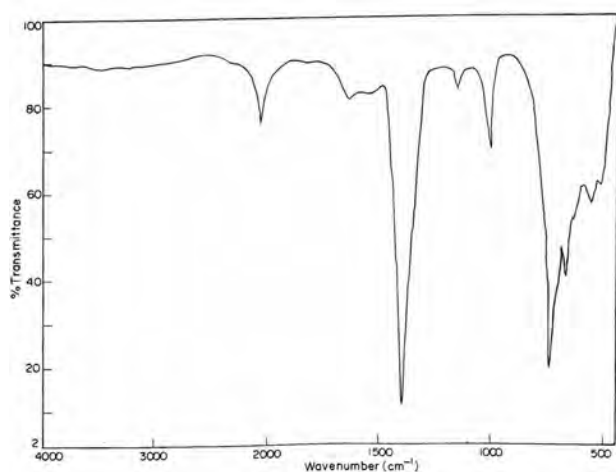


Fig. 2: FTIR spectrum of MGI crystal

#### 3.3 Optical Absorption Studies

The optical absorption spectrum of MGI was recorded between 200 and 2000 nm. The absorption curve is shown in Fig. 3. It is observed from the spectrum that MGI has a wide optical transmission window from 310 nm to 1400 nm. There are no abnormal peaks are observed in this region. It is also noted from the spectrum that MGI crystal cut-off wavelength lies near 310 nm. The graph has been plotted to estimate the direct band gap values using Tauc's relation is shown in Fig. 4. The direct band gap energy of MGI is found to be 3.96 eV.

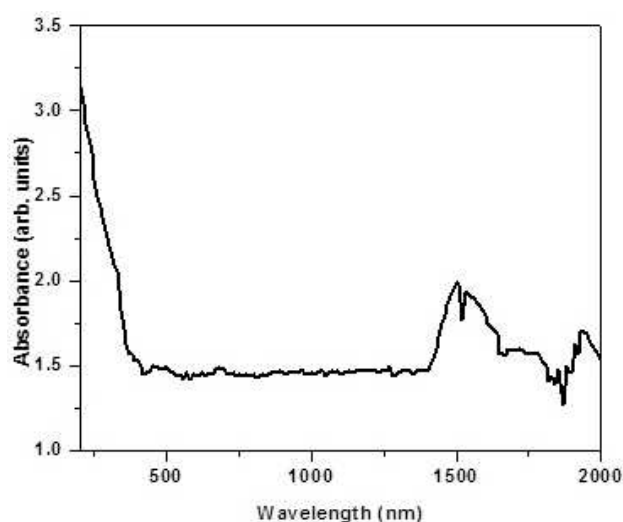


Fig. 3: Optical absorption spectrum of MGI crystal

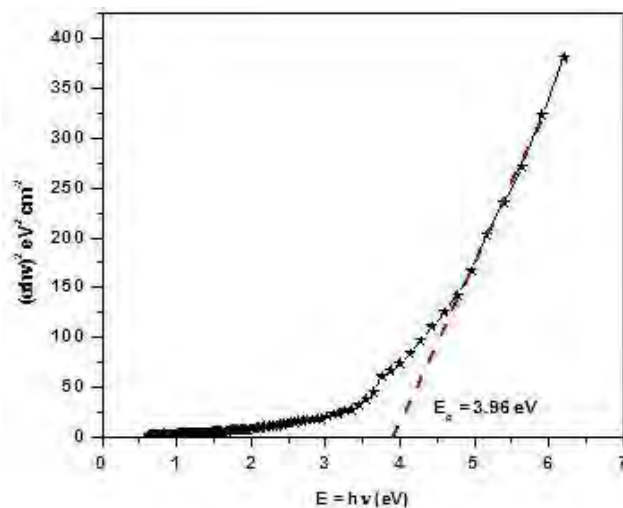


Fig. 4: Tauc's plot of MGI crystal

### 3.4 Kurtz and Perry Powder SHG Test

The nonlinear optical property of the grown crystal was tested by passing a Q-switched mode locked Nd:YAG laser of 1064 nm and pulse width 8 ns on the powder sample of MGI. The input laser beam was passed through an IR reflector and then directed on the microcrystalline powdered sample. Photodiode detector and oscilloscope assembly detected the light emitted by the sample.

The SHG efficiency of the MGI crystal was evaluated by taking the microcrystalline powder KDP as the reference material. For the laser input pulse of 5.6 mJ/pulse, SHG signal of 160 mV and 620 mV were obtained for KDP and MGI samples respectively. Hence, it is observed that the SHG efficiency of MGI is nearly four times than KDP.

### 3.5 Microhardness Studies

The selected surface of the MGI single crystal was taken to measure the hardness value for applied loads of 10, 25, 50 and 100 g. The static indentations were made at room temperature with a constant indentation time of 10 seconds. The variations of Vickers hardness number ( $H_v$ ) with applied loads ( $p$ ) are shown in Fig. 5. It is inferred from the figure that the hardness of MGI was decreased with increasing loads. For an indentation load of 100 g, cracks were initiated on the crystal surface around the indenter, which is due to

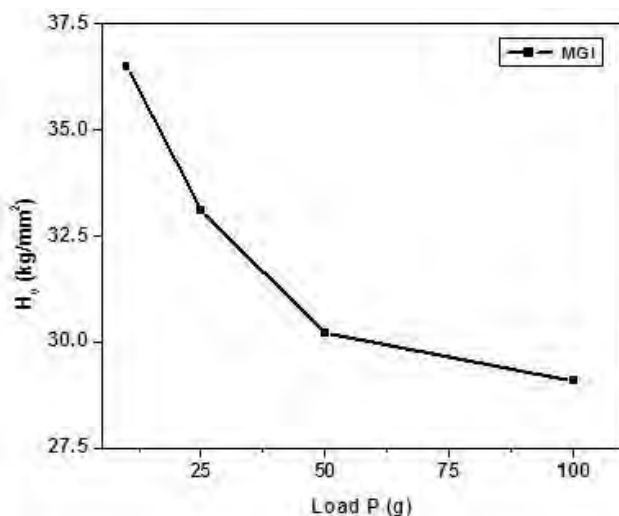


Fig. 5:  $H_v$  values Vs applied load of MGI crystal

the release of internal stress locally initiated by indentation. By plotting  $\log p$  vs  $\log d$  (Fig. 6), the value of work hardening coefficient ( $n$ ) was calculated as 1.814. Since the value of  $n$  is lesser than 2, the hardness measurement reveals that the grown crystal belongs to hard category material [15].

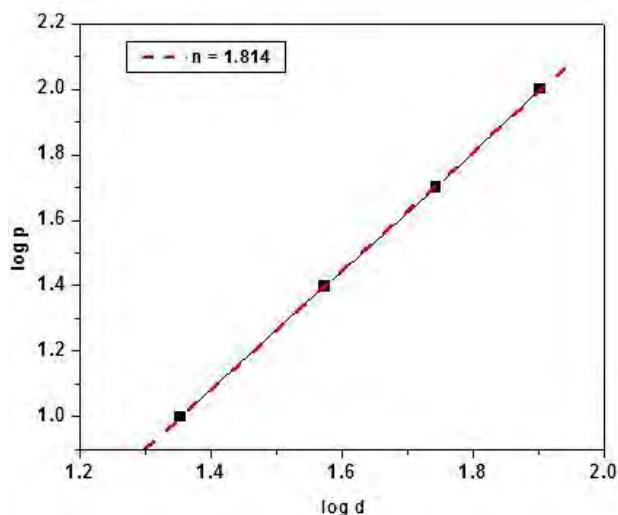


Fig. 6: Plot of  $\log p$  Vs  $\log d$  of MGI crystal

### 3.6 Thermal Studies

In TGA curve (Fig. 7), no weight loss is observed up to 650°C which reflects the thermal stability of the grown crystal. There is a single stage weight loss between 820 to 1060°C ascribed to the decomposition of the compound. It is expected that the breaking of molecules like iodine and oxygen from  $Mg(IO_3)_2$  compound occur in the stage of decomposition. The thermal stability of MGI is found to be superior to other iodate crystals like  $Zn(IO_3)_2$  (580°C),  $Mn(IO_3)_2$  (480°C),  $\beta$ - $Ni(IO_3)_2$  (580°C) and  $Ca(IO_3)_2$  (550°C) [14 & 16].

### 3.7 Dielectric Studies

Fig. 8 shows the variation of dielectric constant as a function of frequency for different temperatures. At low frequencies, the dielectric constant is found to be a maximum and it decreases with increasing frequency and after reaching a frequency of 5 kHz, the dielectric constant remains constant at a value of

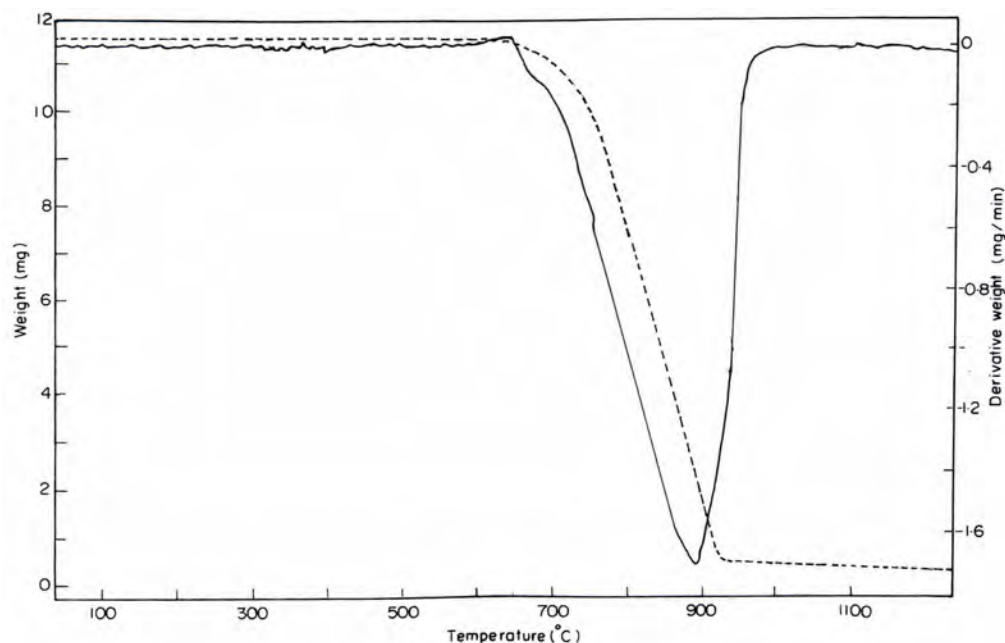


Fig. 7: TG-DTG curves of MGI crystal

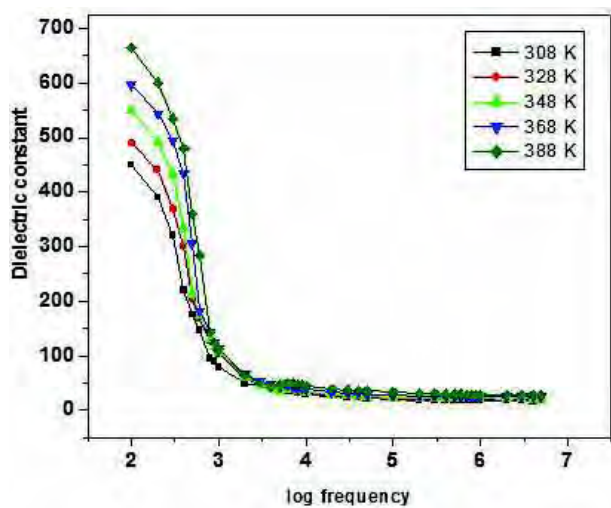


Fig. 8: Variation of dielectric constant with log frequency at different temperature

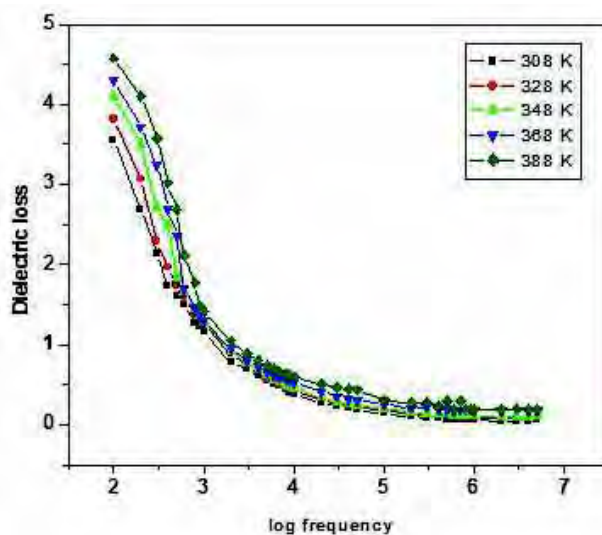


Fig. 9: Variation of dielectric loss with log frequency at different temperature

35.12 with further increase in frequency. The higher value of dielectric constant at low frequency may be attributed to space charge polarization.

The exponential decrease of dielectric loss with frequency is also shown in Fig. 9. The characteristics of low dielectric loss with high frequency for MGI suggest that the samples possess enhanced optical

quality with lesser defects and these parameters is of vital importance of nonlinear optical materials in their applications [17]. In space charge polarization the increase of temperature facilitates the diffusion of ions. This leads to the increase in the values of dielectric constant and dielectric loss with increase of temperature.



#### 4. Conclusion

7 x 6 x 3 mm<sup>3</sup> size of MGI crystal was grown by slow cooling method. Unit cell parameters of MGI are  $a = 10.948 \text{ \AA}$ ,  $b = 5.117 \text{ \AA}$ ,  $c = 10.945 \text{ \AA}$ ,  $\alpha = \beta = 90^\circ$  and  $\gamma = 120^\circ$  from single crystal XRD. The various functional groups of MGI crystal are identified by FTIR spectrum. Optical cut-off wavelength of the sample is observed as 310 nm which augurs well as a property for NLO application. The microhardness

measurements prove that MGI belongs to the hard category of materials. MGI exhibits higher SHG efficiency than the potassium dihydrogen phosphate (KDP) and these crystals can be promising materials for nonlinear device fabrication. TG-DTG curve shows the crystal has no weight loss upto 650°C which reflects the thermal stability of the grown crystal. Dielectric studies show that the grown crystal possesses space charge polarization and less defects.

#### References

1. Sagawa M, Kagawa H, Kakuta A, Kaji M, Saeki M and Namba Y *Appl Phys Lett* **66** (1995) 547
2. Kitazawa M, Higuchi R, Takaashi, Wada M and Sasabe H *Appl Phys Lett* **64** (1994) 2477
3. Yamamoto H, Funato S, Suglyama T, Johnson RE, Norwood RA, Jung J, Kinoshita T and Sasaki K *J Opt Soc Am B* **13** (1996) 837
4. Li ZD, Wu BC, Su GB and Hung GF *Appl Phys Lett* **70** (1997) 562
5. Yuan DR, Xu D, Liu MG, Fang Q, Yu WT, Hou WB, Bing YH, Sun SY and Jiang MH *Appl Phys Lett* **70** (1997) 544
6. Xing GC, Jiang MH and Shao ZS *Chinese J Laser* **14** (1987) 302
7. Ginson P Joseph, Philip J, Rajarajan K, Rajasekar SA, Joseph Arul Pragasam A, Thamizharasan K, Ravi Kumar SM and Sagayaraj P *J crystal Growth* **296** (2006) 51
8. Selvakumar S, Ravi Kumar SM, Rajarajan K, Joseph Arul Pragasam AA, Rajasekar SA, Thamizharasan K and Sagayaraj P *Crystal Growth and Design* **6** (2006) 2607
9. Zhang N, Yuan DR, Tao XT, Xu D, Shao ZS and Minhua Jiang *Chinese Sci Bull* **15** (1989) 1154
10. Bergmann JG, Brown GD, Ashkin A and Kurtz SK *J Appl Phys* **40** (1969) 2860
11. Delphine Phanon, Bachir Bentría, Djamal Benbortal, Alain Mosset, Isabelle Gautier-Luneau *Solide State Sciences* **8** (2006) 1466
12. Bachir Bentría, Djamal Benbortal, Muriel Bagieu-Beucher, Alain Mosset, Julien Zaccaro *Solid State Sciences* **5** (2003) 359
13. Bach H *Acta Cryst* **B34** (1978) 263
14. Delphine Phanon, Bachir Bentría, Erwann Jeanneau, Djamal Benberatal, Alain Mosset and Isabelle Gautier-Lunneau, *Z Kristallogr* **221** (2006) 635
15. Onitsch EM *Mikroskopie* **95** (1956) 12
16. Sharda J, Shitole and Saraf KB *Bull Mater Sci* **24** (2001) 461
17. Balarew C and Duhlew R *J Solid state Chem* **55** (1984) 1.